Influence of a Gold Seed in Transparent V_2O_x/Ag/V_2O_x Selective Contacts for Dopant-free Silicon Solar Cells

H.T. Nguyen*, E. Ros*, T. Tom, J. Bertomeu, J.M. Asensi, J. Andreu, I. Martín, P. Ortega, M. Garín, J. Puigdollers, C. Voz, R. Alcubilla

Abstract— **Dielectric/metal/dielectric structures based on vanadium pentoxide with a thin silver interlayer have been optimized to replace traditional transparent electrodes. As would be expected, there is a trade-off in the metal thickness to achieve simultaneously high transparency and low sheet resistance. It has been demonstrated that an ultrathin gold seed prevents the tendency of silver to form clusters. This wetting effect reduces the metal thickness needed to form a continuous film, which leads to a higher averaged transmittance and very low sheet resistance. On the other hand, vanadium pentoxide on silicon forms a high quality hole-selective contact. Thus, these structures can be used as an all-in-one transparent electrode and selective contact for a new kind of heterojunction solar cells. This concept has been proved in a 13.3% efficient solar cell fabricated on n-type silicon wafers. Besides dopant-free, the complete fabrication route did not require any sputtered transparent electrode.**

Index Terms— **Photovoltaic cells, Silicon, Indium tin oxide, Conductivity, Contacts, Silicon, Heterojunctions.**

I. INTRODUCTION

CONCEPTUALLY a solar cell consists of an absorber (semiconductor) sandwiched between two selective contacts, which act as filters for one type of charge-carrier [1]. The exclusive attribution of these filters is their high permeability for one charge-carrier type (electron/hole) while simultaneously blocking the other one. These selective contacts are usually referred in the literature as Electron Transport Layers (ETL) and Hole Transport Layers (HTL), respectively. The use of selective contacts in solar cells was originally developed in emerging PV technologies, such as organic solar cells [2] or, more recently, perovskites solar cells [3]. However, this novel approach also applies to well-established inorganic-based solar cells [4].

Application to crystalline silicon (c-Si) technology is particularly relevant, since it now represents about 90% of global market share [5]. Despite being the most developed and mature technology, efforts to tackle remaining issues are still ongoing. Carrier selectivity in silicon-based solar cells is regularly achieved by doping, which introduces technological complexity. Namely, conventional homojunction solar cells diffused at high-temperature involve an energy-intensive fabrication process. Heterojunction solar cells can be processed at low temperature, but demand hazardous gas precursors. On the other hand, some materials used in new PV technologies have demonstrated excellent charge-carrier selectivity. Thus, the use of such materials substituting standard silicon dopants deserves particular study [6]. In this sense, the use of transition metal oxide (TMO) films on a c-Si absorber has been a success story. Thin films of different TMOs are really good HTLs, they allow an easy hole transport while effectively blocking electrons. Power conversion efficiencies of 22.5% have been achieved on n-type c-Si devices with the use of molybdenum trioxide (MoO_3) as a hole-selective contact [7]. Also remarkable efficiencies exceeding 18% have been reported by using vanadium pentoxide (V_2O_5) and tungsten trioxide (WO3) [8]. This new kind of heterojunction solar cells still use a transparent conductive oxide (TCO) electrode, owing to the high sheet resistance of TMO layers. The high-vacuum Sputtering process to deposit TCO layers tend to generally increase manufacturing costs. Even more important, commonly used tin-doped indium oxide (ITO) electrodes suffer from the high demand of scarce indium element. Particularly, companies manufacturing high added-value flat-panel displays cause price hikes [9]. Therefore, indium-free alternatives to TCO electrodes would be desirable for PV applications.

Over the last years, different TCO/metal/TCO multilayers have been investigated to replace ITO electrodes. These structures can achieve globally better optical and electrical properties compared to a single TCO layer [10]. Tin oxide and either intrinsic or aluminium-doped zinc oxide layers have been used as indium-free TCOs [10–12]. Silver is the most widely used metallic interlayer, although structures with copper and gold have been also reported [13,14]. More

H.T. Nguyen and E. Ros contributed equally to this work.
H.T. Nguyen, E. Ros, I. Martín, P.Ortega, M. Garín, J. Puigdollers, R. Alcubilla and C. Voz are with Universitat Politècnica de Catalunya, Barcelona-08034, Spain (email: thai-ha.nguyen@polytechnique.edu, eloi.ros@upc.edu, pablo.rafael.ortega@upc.edu, moises.garin@upc.edu, joaquim.puigdollers@upc.edu, cristobal.voz@upc.edu ramon.alcubilla@upc.edu) C.Voz is the corresponding author.
T. Tom, J. Bertomeu, J.M. Asensi, J. Andreu are with the Universitat de Barcelona, Barcelona-08034, Spain (email: thomastom@ub.edu, jbertomeu@ub.edu, jmasensi@ub.edu, Jordi.andreu@ub.edu).
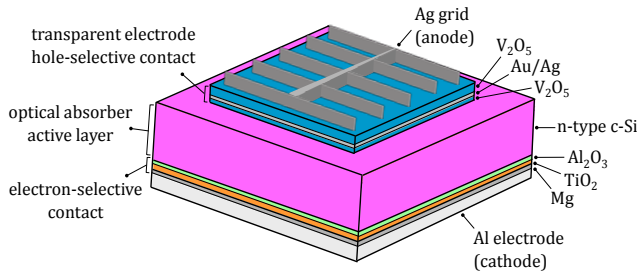
Figure 1. Schematics of the solar cell based on n-type c-Si. The front V_2O_5/Metal/V_2O_5 structure acts as a transparent electrode and hole-selective contact. A dopant-free electron-selective contact is also implemented on the rear side.

recently, dielectric-metal-dielectric (DMD) stacks have been used in organic semiconductor devices [15,16]. In DMD stacks the TCO layers are substituted by semi-insulating films, which very frequently are transition metal oxide layers. The sheet resistance is kept at low values by the metallic layer, while UV transparency can be even higher [17]. All these results point the viability of using TMO-based DMD stacks in crystalline silicon solar cells fulfilling two objectives. First, the bottom TMO layer in contact with silicon determines a strong hole-selective character. Second, the whole DMD structure would operate as an indium-free transparent electrode. This concept has already been implemented as a front MoO_3/Ag/MoO_3 (MAM) selective contact for n-type crystalline silicon solar cells [18]. Different V_2O_5/M/V_2O_5 multilayers (M=Au, Ag, Ca) have also been incorporated in heterojunction-back-contact (HBC) solar cells, although in that case transparency was not a strong requirement [19].

In this work, we study the optical and electrical properties of DMD structures composed of V_2O_5 semi-insulating layers and silver as the intermediate metal. Particularly, a detailed analysis of V_2O_5/Ag/V_2O_5 (VAgV) structures is presented in terms of their quality as a transparent electrode. Additionally, the beneficial effect of intercalating an ultra-thin gold seed is demonstrated in V_2O_5/Au/Ag/V_2O_5 (VAuAgV) multilayers. Vanadium oxide was chosen over other TMO alternatives because it can provide good surface passivation without any interfacial buffer layer [20]. The work was completed by implementing optimized VAuAgV structures as a front hole-selective contact of complete n-type c-Si heterojunction solar cells. A detailed characterization of these devices is presented, which evidences a high-potential for such a cost-effective new heterojunction structure.

II. EXPERIMENTAL

The V_2O_5/Metal/V_2O_5 (VMV) multilayers studied in this work were deposited by thermal evaporation in a vacuum system with base pressure below 10^{-6} mbar. The films were grown at low deposition rates in the range 1-4 Å/s, maintaining the substrates at room temperature. The thickness of the evaporated layers was measured by means of an INFICON SQC-310 deposition controller. It must be considered that quite often very thin layers have not coalesced into homogeneous films. In that case, the thickness measured

by the quartz microbalance must be interpreted just as the amount of material evaporated onto the substrate.

First optical and electrical characterizations were done for VMV structures deposited onto borosilicate glass. These substrates had been previously cleaned in ultrasonic baths of acetone and isopropanol, followed by a thorough deionized water rinse and nitrogen blow until dry. The VMV structures were examined by field-emission scanning electron microscopy (FESEM), focusing on the morphology of ultra-thin metallic layers. The sheet resistance (R_{sh}) was evaluated using a 4-point probe. The optical transmittance was measured using an UV-VIS-NIR Shimadzu 3600 spectrophotometer. These measurements were complemented with calculations of spectral absorption in the silicon wafer obtained by the transfer-matrix method (TMM) [21].

Concerning complete solar cells, these devices were fabricated on polished (100) n-type (2 Ω·cm) c-Si wafers of thickness 280 μm. The VMV structures developed in this work were deposited on the front side to serve as a hole-selective contact as well as transparent electrode. Considering that the VMV structures include ultra-thin layers, we preferred maintaining the c-Si surface flat (non-textured). As a preliminary study, this will allow a more reliable analysis of the results. The low-temperature rear electrode consisted of a stack of aluminium and titanium oxides (Al_2O_3/TiO_2), followed by a magnesium buffer and a final aluminium contact. Such a structure behaves as a good quality dopant-free electron selective contact, as it has been reported in a previous work [22]. The active area of the solar cells (1 cm^2, 4 cm^2) was defined by conventional photolithography and wet-etching steps. Finally, a 2 μm thick Ag grid was thermally evaporated through a shadow mask as a front contact. The metallic grid covered a 4% of the VMV active area. A schematics of the device structure is shown in figure 1. On complete devices, the current density versus voltage (JV) electrical characteristics were measured using a Newport solar simulator and Keithley 2400 DC source-meter. Additionally, quasi-steady-state open-circuit voltage (QSSVoc) measurements [23] were done with a system made in-house. By this technique the actual electrical characteristics can be compared to pseudo JV curves with no influence of the series resistance. Finally, the external-quantum-efficiency (EQE) curves of the solar cells were measured by means of a QEX10 PV Measurements equipment.

III. RESULTS AND DISCUSSION

First, the influence of the metallic layer in the optical properties of VMV structures was investigated. For that purpose, different samples were deposited on glass substrates to measure their optical transmittance. The thicknesses of the bottom and top V_2O_5 layers were fixed at 20 and 35 nm, respectively. As an intermediate metal, we started studying the use of silver layers (M=Ag) with a thickness between 6 and 12 nm. As it can be observed in figure 2, the overall transmittance decreases with the thickness of the intermediate Ag layer. This behaviour could be expected, owing to the optical absorption
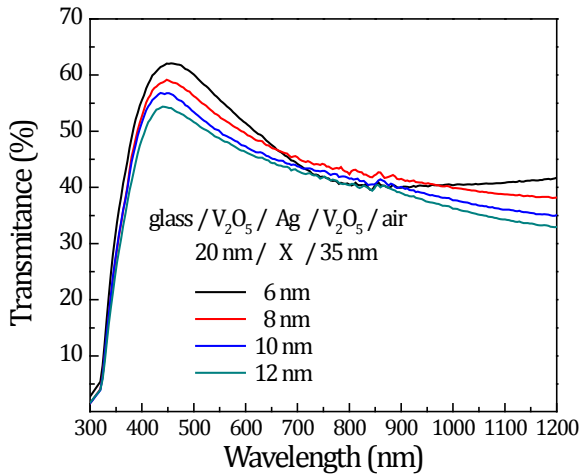
Figure 2. Optical transmittance of V_2O_5/Ag/V_2O_5 (20 nm/X nm/35 nm) samples deposited on glass. As expected, the overall transmittance decreases with the thickness of the intermediate Ag layer. The transmittance of the bare glass substrate is about 92% in the whole measured wavelength range.
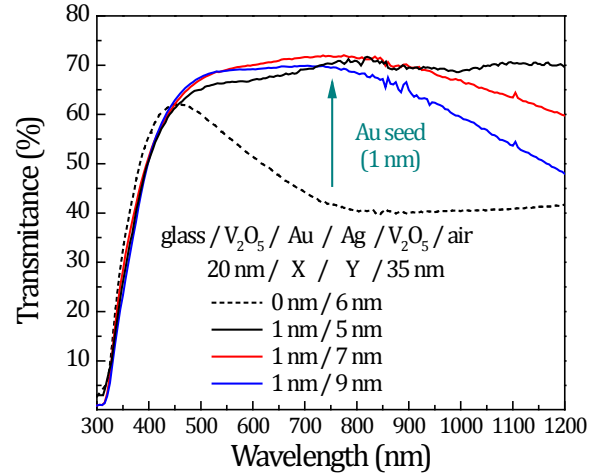

Figure 3. Optical transmittance of V_2O_5/Au/Ag/ V_2O_5 (20 nm/1 nm/X nm/35 nm) samples deposited on glass. A sample with 6 nm thick Ag layer without Au seed is also shown for comparison. The use of a gold seed results in samples of higher transparency.

by the metallic layer. However, transmittance in the infrared region was unexpectedly low for so thin Ag layers. Besides, in the wavelength region 700-900 nm transparency was not in direct correlation to the metal thickness. The characteristic growth of very thin Ag layers might account for this phenomenon. As silver is evaporated onto a dielectric substrate, isolated islands tend to form for the first few nanometers (Volmer-Weber growth) [24]. The absorption caused by the formation of localized surface plasmons would explain the relatively low optical transmittance [25]. An equivalent behaviour has been reported for other DMD structures, where silver was also used as an intermediate metal [26]. The initial formation of islands is explained because Ag atoms prefer bonding each other rather than to the substrate. In this sense, the nominal thickness would be only a reference value for the amount of evaporated metal. A successful approach to promote the formation of a continuous film (Frank-Van der Merwe growth) consists in using a seed (wetting) layer [27,28]. In this work, our choice was to evaporate an ultra-thin (1 nm) gold seed preceding the Ag layer. The dissociation energy of the Au-Ag bond (202.9 kJ/mol) is higher than that of a diatomic Ag-Ag bond (160.3 kJ/mol) [29]. Thus, impinging Ag atoms are expected to bond tightly on the gold seed rather than migrate over the surface to form clusters. Then, a series of VAuAgV multilayers were prepared to compare their characteristics to the previously studied VAgV structures. The Au seed layer (1 nm) was combined with 5, 7 and 9 nm Ag layers for total metal thicknesses equivalent to those of VAgV samples (6, 8 and 10 nm). A comparison of the optical transmittance evidences the interest of using a seed layer (Fig. 3). The VAuAgV multilayers were noticeably more transparent in the visible and infrared regions. Only at short wavelengths (λ<400 nm) the optical transmittance was slightly reduced because of the gold layer. Nevertheless, a better use of the solar spectrum by

the VAuAgV multilayers is clear. The wetting effect of the Au seed could be definitely confirmed in the FESEM images (Fig. 4). The left image corresponds to the VAgV sample with 8 nm thick Ag layer, where isolated clusters of silver can be clearly resolved. By contrast, the sample with an intermediate Au/Ag stack (1 nm/7 nm) shows a continuous and much more homogeneous film.

Considering the final intend to fabricate solar cells, not only high transparency but also good electrical properties are needed. Thus, the sheet resistance of the different multilayers was measured by means of a 4-point probe. Figure 5 shows an abrupt drop in the sheet resistance of the VAgV samples when the metal thickness is increased to 10 nm. The samples with Ag layers thinner than 8 nm behaved as insulators of high sheet resistance (R_{sh}~100 $k\Omega_{sq}$). This behaviour can be directly related to the initial Volmer-Weber growth of the silver layer, which results in the earliest formation of isolated islands. Above a nominal thickness those islands coalesce, which reduces the sheet resistance by three orders of magnitude. Similar percolation thresholds have been reported in the literature for MoO_3/Ag/MoO_3 structures, although these values could shift depending on the deposition rate [30]. Among the series of VAgV samples, only those with 10 nm (87 Ω_{sq}) and 12 nm (30 Ω_{sq}) metal layers have good R_{sh} values to fabricate solar cells. By contrast, all the VAuAgV layers evidenced rather low R_{sh} values starting from 97 Ω_{sq} for the thinnest Au/Ag metallic stack (1 nm/5 nm). The sheet resistance steadily decreases to values as low as 29 Ω_{sq} (1 nm/7 nm) and 5 Ω_{sq} (1 nm/9 nm) for thicker Ag layers. On the other hand, any of the VAuAgV samples presented average transmittances a 10-15% higher than those of standard VAgV structures with equivalent metal thickness (Fig. 5 inset). All these results outline the convenience to use an adequate seed in structures based on silver as its main metallic layer.

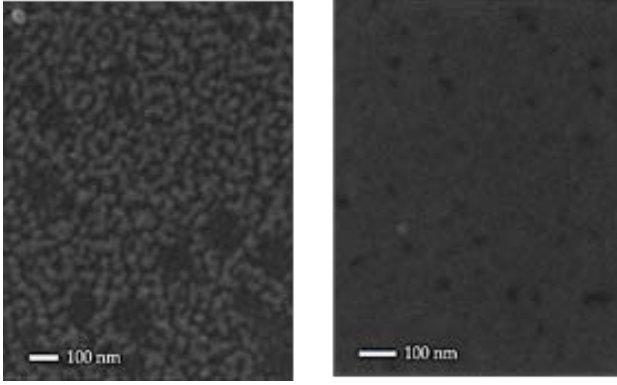At this point, we must remember the prime objective to

Figure 4. Comparison of FESEM images for VAgV (left) and VAuAgV samples (right). The use of a gold seed results in more homogeneous films, whereas multiple clusters can be observed for the VAgV image.

develop an all-in-one selective-contact plus transparent electrode for silicon-based solar cells. Thus, these multilayers should be actually tuned for their best optical performance on a c-Si substrate. For that purpose, we used the TMM algorithm to calculate the wavelength-dependent absorption (A) of a Si wafer coated by different VAuAgV structures. The optical parameters (refractive index and extinction coefficient) of the different layers were taken from the literature [31,32]. Then, the total photogenerated current (J_{ph}) was evaluated by integrating the air-mass 1.5 global irradiance ($AM1.5$) properly weighted by the absorptance spectra in the Si wafer:

$$J_{ph} = \int_0^{hc/E_g} A(\lambda)\ \frac{q\lambda}{hc}\ AM1.5(\lambda)\ d\lambda \qquad (1)$$

Figure 6 shows the results of this analysis for a fixed 10 nm thick Ag interlayer, varying both the top and bottom V$_2$O$_5$ layer thicknesses. In order to achieve a good hole-selective character, the bottom V$_2$O$_5$ layer should be around 20 nm thick [20]. Thus, an adequate thickness for the top V$_2$O$_5$ layer that minimizes reflection losses would be around 50-60 nm. This value did not shift very significantly when the same analysis (not shown) included a thin (1 nm) Au seed or the Ag thickness was varied from 6 to 10 nm.
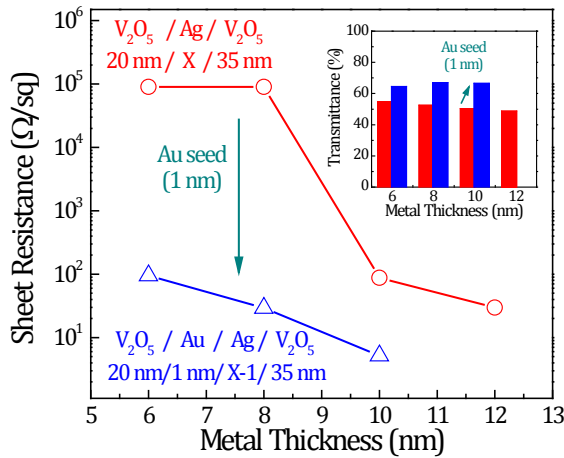

Figure 5. Sheet resistance as a function of the metal thickness for both VAgV and VAuAgV series of samples. The gold seed favours a fast percolation for very thin metal layers, which can reduce the sheet resistance several orders of magnitude. The smooth nanostructure also limits the absorption of localized surface plasmons, which results in more transparent samples (inset).
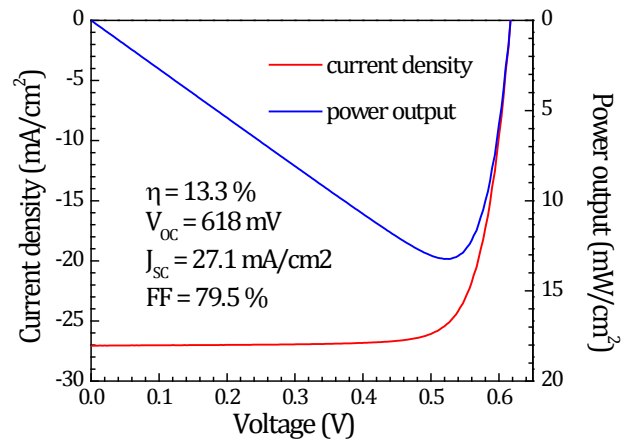

Figure 7. JV curve (left axis) and power output (right axis) measured under AM1.5 irradiance (100 mW/cm^2). The high FF of 79.5% confirms the high quality of the VAuAgV structure as an indium-free transparent electrode.

This work finished by fabricating complete solar cells implementing an optimized VAuAgV multilayer on the front side. The thickness for the bottom V_2O_5 layer was 20 nm, which ensures a strong hole-selectivity on the Si absorber. The metallic interlayer consisted of a 1 nm thick Au seed followed by a 7 nm thick Ag layer. Finally, a top V_2O_5 layer (55 nm) coated the metallic stack to reduce reflection losses. These values were chosen for the best solar cell performance, in accordance with all the studies done in this work. The final device yielded a 13.3% conversion efficiency (η) under a simulated AM1.5 irradiance of 100 mW/cm^2. The photovoltaic parameters of the JV curve were J_{sc}=27.1 mA/cm2, V_{oc}=618 mV and FF=79.5 % (Fig. 7). The open-circuit voltage was remarkably high compared to that of a similar device (V_{oc}=583 mV) with a $MoO_3/Ag/MoO_3$ front contact [18]. Such a difference might be explained by the superior performance of silicon heterojunctions based on V_2O_5 over other transition-metal-oxide alternatives [8][20]. Nevertheless, the final V_{oc} values could be also influenced by the particular rear contact implementation. On the other hand, it is noticeable the high FF value of the solar cell presented here. The low sheet resistance achieved with the Au/Ag stacks could be the main factor contributing to that good result. In this regard, the quasi-steady-state V_{oc} curve of the device was measured as a function of the illumination intensity. These data were used calculate a pseudo-JV curve in which the effect of the series resistance is eliminated (Fig. 8). The corresponding pseudo-FF (pFF) increases to 81.6%, which points to a good quality diode. Actually, the exponential region of the pseudo-JV curve could be fitted by considering a single-diode model:

$$J = J_o\left(e^{qV/nkT} - 1\right) \qquad (2)$$

with a low saturation current density $J_o = 4.8 \ pA/cm^2$ and rather good (close to one) ideality factor $n = 1.1$). The value
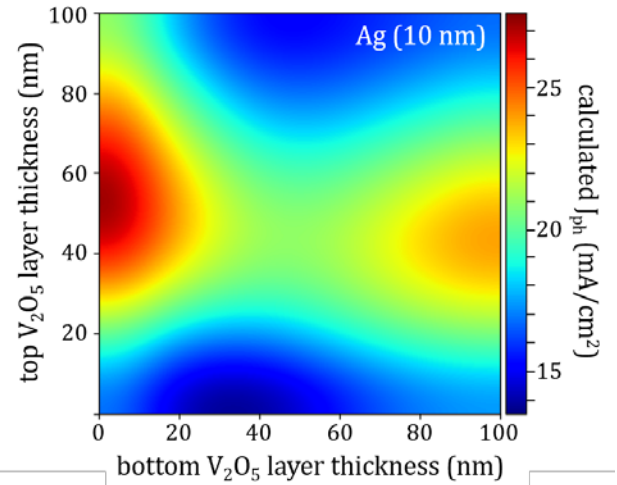
Figure 6. Mapping of the photogenerated current under AM1.5 irradiance as a function of the top and bottom V_2O_5 layer thicknesses. In this case, the thickness of the silver layer was fixed at 10 nm. The bottom layer should be around 20 nm thick to have good hole-selectivy. Thus, a top V_2O_5 layer of about 50-60 nm would provide good antireflection properties.

of the total series resistance (R_S) can be obtained from the pFF and the parameters of the JV curve under illumination following [33]:

$$R_S = \frac{V_{oc}}{J_{sc}}\left(1 - \frac{FF}{pFF}\right) \qquad (3)$$

this calculation results in a R_S value as low as 0.6 $\Omega \cdot cm^2$, which proves the good electrical quality of optimized VAuAgV electrodes.

The moderate J_{sc} value is the main factor limiting the efficiency of this solar cell structure. Figure 9 shows the external-quantum-efficiency (EQE) curve of the solar cell together with its front reflectance spectra. In the inset, charge-carrier generation and different loss mechanisms are balanced for an AM1.5 irradiance. The incident photons with energy higher than the Si bandgap could generate a maximum photocurrent of 42.3 mA/cm^2. Reflection on the front surface causes a 16.7% loss, which limits the photogenerated current to approximately 35.2 mA/cm^2. The measured EQE curve implies a 23% internal loss, which results in a final J_{sc} value of 27.1 mA/cm^2. This reduction could be explained by considering the optical absorption of the VAuAgV structure, mainly at its metallic stack. Internal charge-carrier recombination also reduces the J_{sc} value, but less significantly because of the good quality c-Si absorber and the use of a passivated rear contact. All the samples and solar cells studied in this work were fabricated on flat substrates. Assuming that internal losses should remain similar, the use of textured substrates could lead to J_{sc} values of about 30 mA/cm^2. Furthermore, according to the electrical characterisation (Fig. 5), the Au/Ag stack could be thinned below 6 nm maintaining R_{sh} values in the range of 10^2 Ω_{sq}. In combination with an optimised metallisation scheme, this change would increase the J_{sc} value by 3-4 mA/cm^2 without a significant FF degradation.
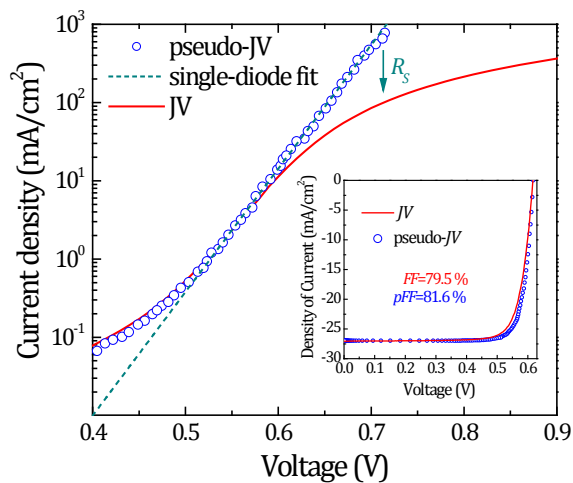
Figure 8. Dark JV of the solar cell compared to its pseudo-JV curve deduced from quasi-steady-state V_{oc} measurements. The inset compares the electrical characteristics under illumination. The high pFF of 81.6% evidences the quality of the selective contacts implemented in this solar cell structure.

IV. CONCLUSION

Traditional transparent-conductive-oxide electrodes can be replaced by optimized stacks of V_2O_5/metal/ V_2O_5 layers. This approach circumvents the scarcity of indium, which could limit the viability of widely used ITO electrodes. Furthermore, the evaporation of these layers is more gentle to the underlying interface compared to the sputtering technique. The sheet resistance of VMV structures clearly improves that of standard TCO electrodes, although the averaged transmittance is slightly reduced. In this sense, a minimum Ag thickness of 10 nm is required to achieve low R_{sh} values. However, the use of an ultrathin Au seed (1 nm) favours that Ag layers as thin as 6 nm already coalesce into a continuous film. The reduction in the thickness of the intermediate metallic layer increases the optical transmittance by more than 15%. Given the hole-selective character of V_2O_5 layers on silicon, fabrication of dopant-free heterojunction solar cells is straightforward. In this work, an optimized $V_2O_5/Au/Ag/V_2O_5$ structure on n-type c-Si yielded a conversion efficiency of 13.3%. The remarkably high fill-factor (79.5%) points out the low sheet resistance achieved with this alternative transparent electrode. The open-circuit voltage (618 mV) is also rather good, even more considering that it is likely limited by the also novel rear contact implemented here. There is definitely room for improvement in the J_{sc} value (27.1 mA/cm2). In this sense, technological transfer to textured substrates could be the next step for this research line.

REFERENCES

[1] P. Würfel, *Physics of Solar Cells: From Basic Principles to Advanced Concepts,* Wiley-VCH, Weinheim, 2009.

[2] M. Riede, T. Mueller, W. Tress, R. Schueppel, K. Leo, "Small-molecule solar cells - Status and perspectives", *Nanotechnology.* 19 (2008). doi:10.1088/0957-4484/19/42/424001.

[3] E.J. Juarez-Perez, M. Wußler, F. Fabregat-Santiago, K. Lakus-Wollny, E. Mankel, T. Mayer, W. Jaegermann, I. Mora-Sero, "Role of the Selective Contacts in the Performance of Lead Halide Perovskite Solar Cells", *J. Phys. Chem. Lett.* 5 (2014) 680–685. doi:10.1021/jz500059v.

[4] U. Wurfel, A. Cuevas, P. Wurfel, "Charge Carrier Separation in Solar Cells," *IEEE J. Photovoltaics.* 5 (2015) 461–469. doi:10.1109/JPHOTOV.2014.2363550.

[5] K. Sopian, S.L. Cheow, S.H. Zaidi, "An overview of crystalline silicon solar cell technology: Past, present, and future," in: *AIP Conference Proceedings*, 2017: p. 020004. doi:10.1063/1.4999854.

[6] P. Gao, Z. Yang, J. He, J. Yu, P. Liu, J. Zhu, Z. Ge, J. Ye, "Dopant-Free and Carrier-Selective Heterocontacts for Silicon Solar Cells: Recent Advances and Perspectives", *Adv. Sci.* (2017) 1700547. doi:10.1002/advs.201700547.

[7] J. Geissbühler, J. Werner, S. Martin De Nicolas, L. Barraud, A. Hessler-Wyser, M. Despeisse, S. Nicolay, A. Tomasi, B. Niesen, S. De Wolf, C. Ballif, "22.5% efficient silicon heterojunction solar cell with molybdenum oxide hole collector", *Appl. Phys. Lett.* 107 (2015) 081601. doi:10.1063/1.4928747.

[8] M. Bivour, J. Temmler, F. Zahringer, S. Glunz, M. Hermle, "High work function metal oxides for the hole contact of silicon solar Cells," in: 2016 *IEEE 43rd Photovolt. Spec. Conf.*, IEEE, 2016: pp. 0215–0220. doi:10.1109/PVSC.2016.7749581.

[9] R.L. Moss, E. Tzimas, H. Kara, P. Willis, J. Kooroshy, "Critical Metals in Strategic Energy Technologies," *Publications Office of the European Union*, Luxembourg, 2011. doi:10.2790/35600.

[10] S. Yu, W. Zhang, L. Li, D. Xu, H. Dong, Y. Jin, "Optimization of SnO2/Ag/SnO2tri-layer films as transparent composite electrode with high figure of merit," *Thin Solid Films.* 552 (2014) 150–154. doi:10.1016/j.tsf.2013.11.109.

[11] S. Vedraine, A. El Hajj, P. Torchio, B. Lucas, "Optimized ITO-free tri-layer electrode for organic solar cells," *Org. Electron.* 14 (2013) 1122–1129. doi:10.1016/j.orgel.2013.01.030.

[12] G. Torrisi, I. Crupi, S. Mirabella, A. Terrasi, "Robustness and electrical reliability of AZO/Ag/AZO thin film after bending stress," *Sol. Energy Mater. Sol. Cells.* 165 (2017) 88–93. doi:10.1016/j.solmat.2017.02.037.

[13] S. Song, T. Yang, M. Lv, Y. Li, Y. Xin, L. Jiang, Z. Wu, S. Han, "Effect of Cu layer thickness on the structural, optical and electrical properties of AZO/Cu/AZO tri-layer films," *Vacuum.* 85 (2010) 39–44. doi:10.1016/j.vacuum.2010.03.008.

[14] T. Dimopoulos, G.Z. Radnoczi, B. Pécz, H. Brückl, "Characterization of ZnO:Al/Au/ZnO:Al trilayers for high performance transparent conducting electrodes," *Thin Solid Films*. 519 (2010) 1470–1474. doi:10.1016/j.tsf.2010.09.049.

[15] S.-W. Liu, T.-H. Su, P.-C. Chang, T.-H. Yeh, Y.-Z. Li, L.-J. Huang, Y.-H. Chen, C.-F. Lin, "ITO-free, efficient, and inverted phosphorescent organic light-emitting diodes using a WO3/Ag/WO3 multilayer electrode," *Org. Electron.* 31 (2016) 240–246. doi:10.1016/j.orgel.2016.01.035.

[16] M. Baishakhi Upama, M. Wright, N. Kumar Elumalai, M. Arafat Mahmud, D. Wang, K. Howe Chan, C. Xu, F. Haque, A. Uddin, "High performance semitransparent organic solar cells with 5% PCE using non-patterned MoO3/Ag/MoO3 anode," *Curr. Appl. Phys.* 17 (2017) 298–305. doi:10.1016/j.cap.2016.12.010.

[17] A.T. Barrows, R. Masters, A.J. Pearson, C. Rodenburg, D.G. Lidzey, "Indium-free multilayer semi-transparent electrodes for polymer solar cells," *Sol. Energy Mater. Sol. Cells* 144 (2015) 600-607. doi:10.1016/j.solmat.2015.10.010.

[18] W. Wu, J. Bao, Z. Liu, W. Lin, X. Yu, L. Cai, B. Liu, J. Song, H. Shen, "Multilayer MoOx/Ag/MoOx emitters in dopant-free silicon solar cells," *Mater. Lett.* 189 (2017) 86–88. doi:10.1016/j.matlet.2016.11.059.

[19] W. Wu, W. Lin, J. Bao, Z. Liu, B. Liu, K. Qiu, Y. Chen, H. Shen, "Dopant-free multilayer back contact silicon solar cells employing V_2O_x /metal/V_2O_x as an emitter," *RSC Adv.* 7 (2017) 23851–23858. doi:10.1039/C7RA03368K.

[20] O. Almora, L.G. Gerling, C. Voz, R. Alcubilla, J. Puigdollers, G. Garcia-Belmonte, "Superior performance of V2O5 as hole selective contact over other transition metal oxides in silicon heterojunction solar cells," *Sol. Energy Mater. Sol. Cells.* 168 (2017) 221–226. doi:10.1016/j.solmat.2017.04.042.

[21] C.C. Katsidis, D.I. Siapkas, "General transfer-matrix method for optical multilayer systems with coherent, partially coherent, and incoherent interference," *Appl. Opt.* 41 (2002) 3978. doi:10.1364/AO.41.003978.

[22] G. Masmitjà, P. Ortega, J. Puigdollers, L.G. Gerling, I. Martín, C. Voz, R. Alcubilla, "Interdigitated back-contacted crystalline silicon solar cells with low-temperature dopant-free selective contacts," *J. Mater. Chem. A.* 6 (2018) 3977–3985. doi:10.1039/C7TA11308K.

[23] M.J. Kerr, A. Cuevas, R.A. Sinton, "Generalized analysis of quasi-steady-state and transient decay open circuit voltage measurements," J. Appl. Phys. 91 (2002) 399. doi: 10.1063/1.1416134

[24] M. Ohring, *Materials science of thin films: deposition and structure*, Academic Press, 2002.

[25] R. Pandey, B. Angadi, S.K. Kim, J.W. Choi, D.K. Hwang, W.K. Choi, "Fabrication and surface plasmon coupling studies on the dielectric/Ag structure for transparent conducting electrode applications," *Opt. Mater. Express.* 4 (2014) 2078. doi:10.1364/OME.4.002078.

[26] M. Wu, S. Yu, L. He, L. Yang, W. Zhang, "High quality transparent conductive Ag-based barium stannate multilayer flexible thin films," *Sci. Rep.* 7 (2017) 103. doi:10.1038/s41598-017-00178-9.

[27] L. Logeeswaran VJ, N.P. Kobayashi, M.S. Islam, W. Wu, P. Chaturvedi, N.X. Fang, S.Y. Wang, R.S. Williams, "Ultrasmooth Silver Thin Films Deposited with a Germanium Nucleation Layer," *Nano Lett.* 9 (2009) 178–182. doi:10.1021/nl8027476.

[28] N. Formica, D.S. Ghosh, A. Carrilero, T.L. Chen, R.E. Simpson, V. Pruneri, "Ultrastable and Atomically Smooth Ultrathin Silver Films Grown on a Copper Seed Layer," *ACS Appl. Mater. Interfaces.* 5 (2013) 3048–3053. doi:10.1021/am303147w.

[29] J.A. Kerr, D.A. Stocker, Handbook of Chemistry and Physics, 87th ed., CRC Press, Devon U.K., 2007.

[30] L. Cattin, Y. Lare, M. Makha, M. Fleury, F. Chandezon, T. Abachi, M. Morsli, K. Napo, M. Addou, J.C. Bernède, "Effect of the Ag deposition rate on the properties of conductive transparent MoO_3/Ag/MoO_3 multilayers," *Sol. Energy Mater. Sol. Cells.* 117 (2013) 103-109. doi:10.1016/j.solmat.2013.05.026.

[31] P.B. Johnson, R.W. Christy, "Optical Constants of the Noble Metals," *Phys. Rev. B.* 6 (1972) 4370–4379. doi:10.1103/PhysRevB.6.4370.

[32] S. Thiagarajan, M. Thaiyan, R. Ganesan, "Physical property exploration of highly oriented V_2O_5 thin films prepared by electron beam evaporation," *New J. Chem.* 39 (2015) 9471–9479. doi:10.1039/C5NJ01582K.

[33] A.L. Fahrenbruch and R.H. Bube, *Fundamentals of Solar Cells.* New York: Academic, 1983.